Large Modulation of Bottlebrush Diblock Copolymer Morphology and Structural Color through Solvent Selectivity

Sanghyun Jeon,[1] Yash Kamble,[2] Zhuang Xu,[3] Azzaya Khasbaatar,[2] Changhyun Hwang,[2] Jong-Hoon Lee,[2] Jiachun Shi, [2] Simon A. Rogers, [2,4] Damien Guironnet,[2,3,4] Ying Diao*[2,4]

[1]Department Materials Science and Engineering, University of Illinois at Urbana-Champaign, 1304 W Green St, Urbana, IL 61801, USA

[2]Department of Chemical and Biomolecular Engineering, University of Illinois at Urbana-Champaign, 600 South Mathews Avenue, Urbana, Illinois 61801, USA

[3]Department of Chemistry, University of Illinois at Urbana-Champaign, 505 S Mathews Ave, Urbana, IL 61801, USA

[4]Beckman Institute for Advanced Science and Technology, University of Illinois at Urbana-Champaign, 405 N. Mathews Ave. M/C 251, Urbana, Illinois 61801, USA

KEYWORDS. Bottlebrush block copolymer, Self-assembly, Solvent selectivity, Structural color, Photonic crystal

*Correspondence to: yingdiao@illinois.edu

Material Synthesis

    (I)   Procedure for the synthesis of Polystyrene (PS) macromonomers[1]
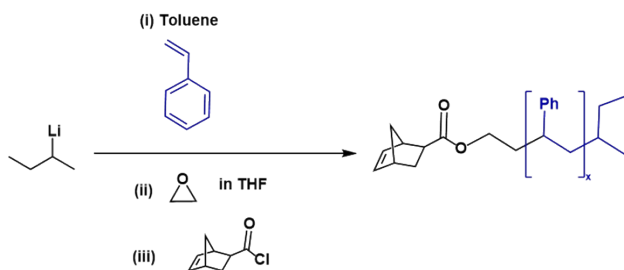
An oven-dried 500 mL round bottom flask was filled with 220 ml of dried toluene. Styrene (18.3 g, 176 mmol) was added next, followed by the sec-BuLi (3 ml, 3.9 mmol) solution to initiate the polymerization. The reaction mixture immediately turned deep orange. After 30 min, ethylene oxide solution (1.95 ml, 5.85 mmol) was added, which immediately resulted in the solution going colorless. After 30 min, exo-5-norobornene-2-acid chloride (794 mg, 5.07 mmol) was added. The reaction was allowed to stir overnight, in which a small amount of white solid formed. The polymer was isolated by precipitation in methanol and dried under vacuum.

$M_{n, GPC}$ = 4,800 g/mol; Đ = 1.03

    (II)   Procedure for the synthesis of Poly lactide (PLA) macromonomers[2]
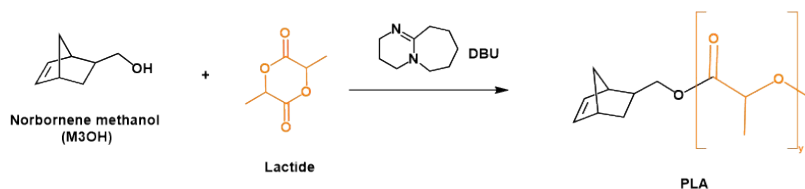
To an oven-dried 20 mL round bottom flask, lactide (1440 mg, 10 mmol, 1.2 ml) and M3OH (31 mg, 0.25 mmol) dissolved in 8.7 mL of THF. The polymerization was initiated by adding DBU (7.6 mg, 0.05 mmol) dissolved in 1 mL of THF. This reaction was mixed till the desired arm length was reached (60 min) at which time $B(OH)_3$ (20 mg, 0.32 mmol) in 2 ml of THF was added to the reaction mixture to quench the reaction. Aliquots were removed for GPC.

$M_{n, GPC} = 5,500 \ g/mol; \ Đ = 1.07$

Note: To get B(OH)$_3$ to dissolve into THF, the solution was heated to 90 °C till all the B(OH)$_3$ dissolved and allowed to cool back to room temperature before use. Avoid rapid cooling of the solution, as it will cause B(OH)$_3$ to drop out of solution.


PS MM   **PS$_m$ BB**
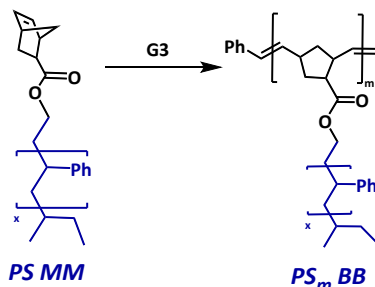
(III)   Synthesis of homopolymer PS bottlebrush polymers

In an oven-dried 20 mL vial, PS macromonomer (1006 mg, 0.24 mmol; 95% norbornene functionalized and $M_{n,PS}$ = 4,200 g/mol) was dissolved into 6.0 mL THF. The polymerization is initiated by adding G3 via a stock solution (0.5 ml add of: 2 mg/mL G3 stock solution). After 15 mins, an aliquot was injected into 1 ml of THF with a large excess of ethyl vinyl ether for GPC analysis. The reaction was quenched by adding a large excess of vinyl ether. The polymer was obtained by precipitating into methanol and dried under vacuum.

Amount of polymer isolated = ~ 890 mg

$M_{n, GPC} = 243 \ kg/mol; \ Đ = 1.17$

*(IV)*   *Synthesis of homopolymer PLA bottlebrush polymers*

PLA
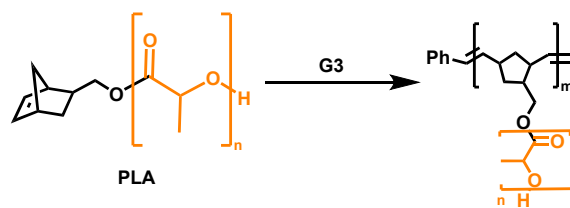
The PLA macromonomers (0.25 mmol; $M_{n,PLA}$ = 4,200 g/mol) were synthesized as mentioned above. The ROMP was initiated by adding G3 via a stock solution (0.55 ml add of: 2 mg/mL G3 stock solution). After 10 mins, an aliquot was injected into 1 ml of THF with a large excess of ethyl vinyl ether for GPC analysis. The reaction was quenched by adding a large excess of vinyl ether. The polymer was obtained by precipitating into methanol and dried under vacuum.

Amount of polymer isolated = ~ 792 mg

$M_{n,\ GPC}$ = 292 kg/mol; Đ = 1.08

(V) Procedure for the graft-through ROMP for the synthesis of PS-b-PLA bottlebrush polymers[1] (Example synthesis for PS$_{200}$-b-PLA$_{200}$)
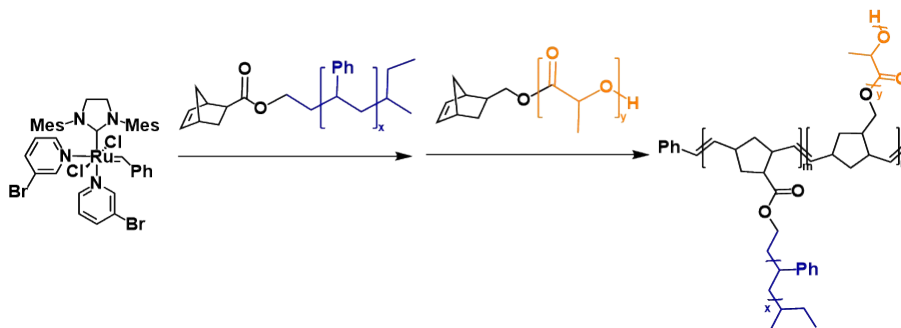
In an oven-dried 20 mL vial, PS macromonomer (1240 mg, 0.25 mmol) was dissolved into 6.9 mL THF. The polymerization is initiated by adding G3 via a stock solution (0.55 ml add of: 2 mg/mL G3 stock solution). After 10 mins, an aliquot was taken and injected into 1 ml of THF with a large excess of ethyl vinyl ether for GPC analysis of the first block. Then, the crude PLA macromonomer from above was added and allow to react for 10 min before a large excess of vinyl ether was added.

The polymer was obtained by precipitating into methanol and dried under vacuum. Amount of polymer isolated = ~ 2 g
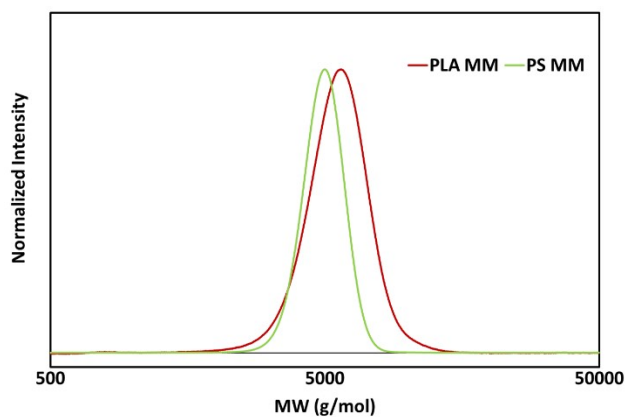
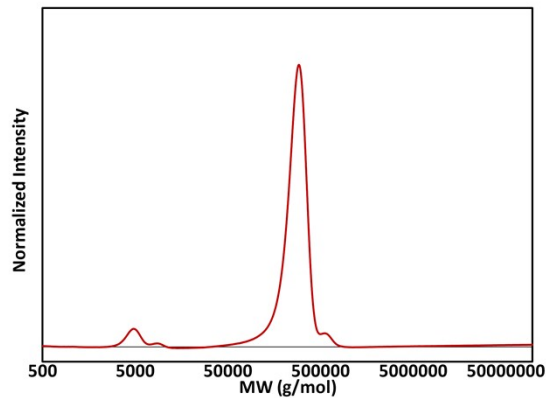**Figure S1:** GPC Trace for PLA and PS Macromonomers

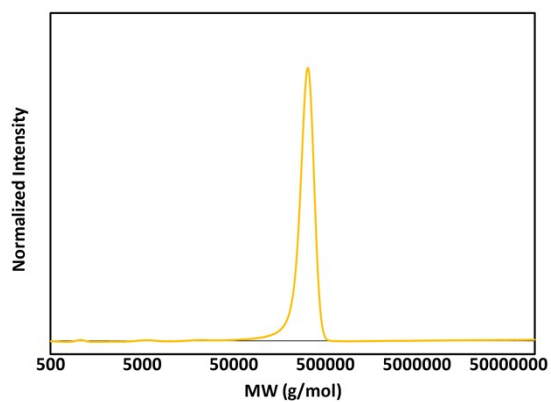**Figure S2:** Synthesis of $PS_{201}^{4.2k}$ homopolymer bottlebrush

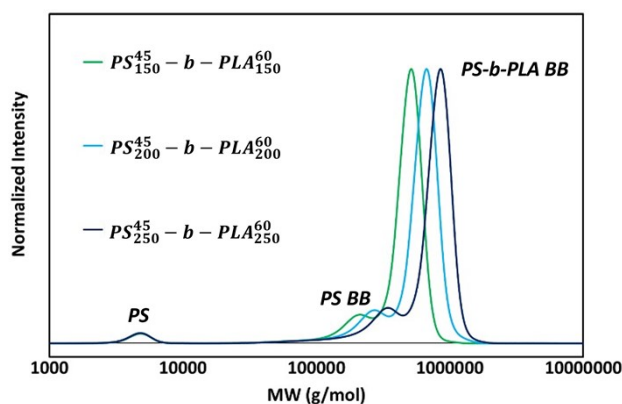**Figure S3:** Synthesis of $PLA_{202}^{4.2k}$ homopolymer bottlebrush

Figure S4: RI-GPC traces for BBCP of varying backbone lengths $PS_{150}^{45} - b - PLA_{150}^{60}$, $PS_{200}^{45} - b - PLA_{200}^{60}$ and $PS_{250}^{45} - b - PLA_{250}^{60}$. The GPC contains three main components: the leftover non-norbornene functionalized PS, homopolymer PS BB and the desired diblock PS-b-PLA BBCP.

N_{bb}	M_n[a] (kg/mol)	M_w/M_n[a]	Macromonomer conversion[b]	wt%[c]			Block length PS: PLA
				Diblock BB	Block 1	PS Brush	
150:150	385	1.2	> 98 %	91	9	< 1%	150:181
200:200	513	1.2	> 98 %	90	10	< 1%	200:247
250:250	635	1.2	> 98 %	90	10	< 1%	250:313
[a] Calculated with respect to PS standards; [b] Determined from GPC (includes both PS and PLA).							
[c] Based on deconvolution of UV-GPC trace as discussed in previous literature[1]							

Table S1: Characterization data for PS-PLA diblock bottlebrush (PS: 4.5 kg/mol; PLA: 4.3 kg/mol). All GPC data can be found in **Figure S1**, **S2, S3, and S4**.
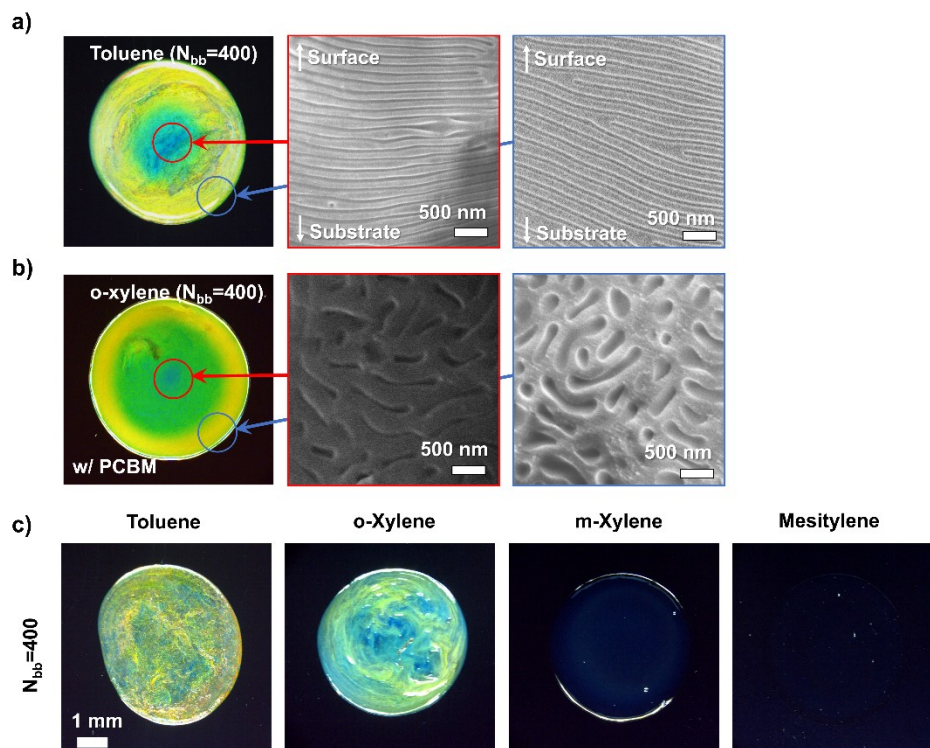
Figure S5. A detailed analysis of the color gradient observed in BBCP (Nbb = 400) samples in **(a)** toluene and **(b)** o-xylene with a broadband absorber is presented. Vertical SEM analysis clearly shows that the center (red) and edge (blue) regions of samples share the same morphologies and orientations, but differ in feature size. The edges exhibit larger features than the center (Toluene: $d_{center} = 159.7 \pm 9.1$ nm, $d_{edge} = 184.3 \pm 8.2$ nm; o-xylene: $d_{NN, center} = 152.1 \pm 17.2$ nm, $d_{NN, edge} = 177.6 \pm 18.3$ nm). **(c)** Optical microscope images of drop-cast samples after solvent vapor annealing, used to relax the structure in each solvent, show that the color gradient disappears post-treatment, indicating that the gradient is triggered by kinetic trapping. This is attributed to the coffee-ring effect during the drop-casting process, which causes a higher concentration at the edges and a lower concentration at the center. During the solvent vapor annealing process, the same solvent used for the initial drop-casting was employed, and the samples were annealed at 60°C

inside a sealed glass container containing a solvent reservoir. Following this treatment, an additional 24-hour annealing step was performed to remove any residual solvent.
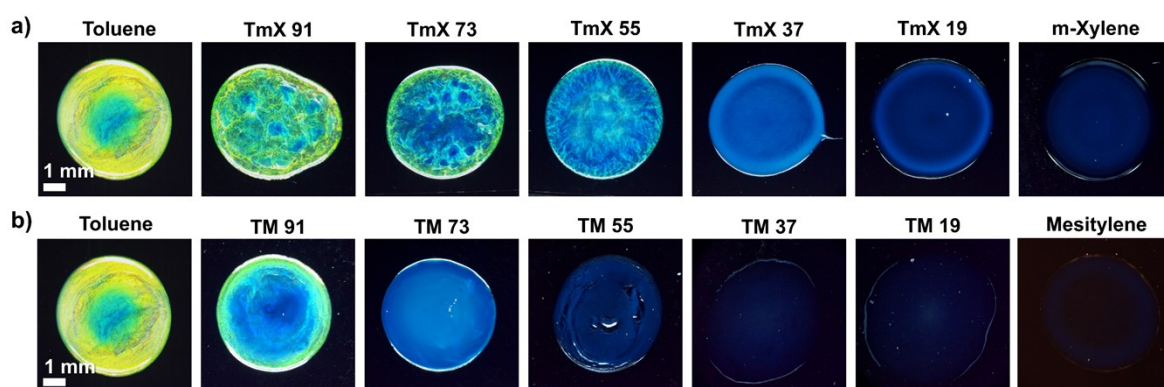
Figure S6. Optical microscope camera images illustrating distinct photonic colors resulting from solvent composition variations: **(a)** toluene and m-xylene mixture, and **(b)** toluene and mesitylene mixture. The numerical notation denotes the volume ratio of each solvent (e.g., TmX 73 = 70v% toluene with 30v% m-xylene).
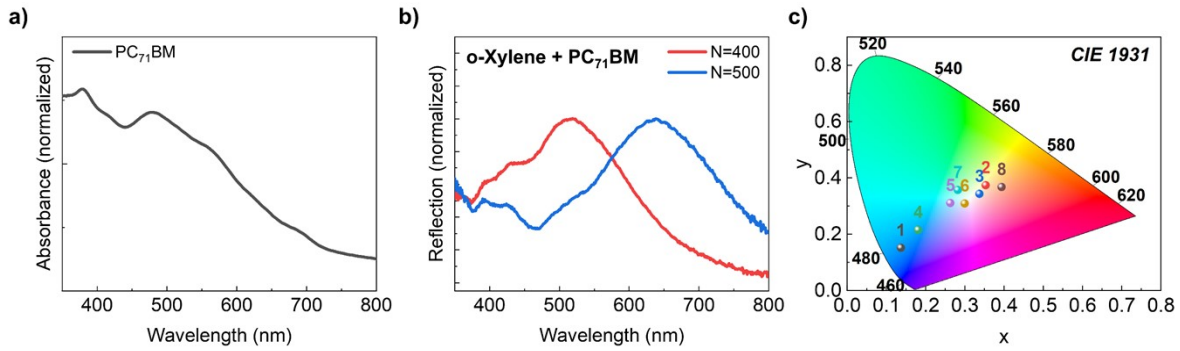
Figure S7. (a) UV-Vis absorption spectra of the broadband absorber ($PC_{71}BM$), and **(b)** diffuse reflection spectra of the BBCP sample (o-xylene, N_{bb}=400, and 500) incorporating 1 wt% of the broadband absorber ($PC_{71}BM$). **(c)** CIE1931 color mapping demonstrating the resultant structural color produced by c-BBCP ink under various conditions of (N_{bb}, solvents): 1 (300, T); 2(400, T); 3(500, T); 4(300, oX); 5(400, oX); 6(500, oX); 7(400, oX+$PC_{71}BM$); 8(500, oX+$PC_{71}BM$). The (x, y) coordinates for each sample are as follows: 1(0.13, 0.15), 2(0.35, 0.38), 3(0.33, 0.34), 4(0.18, 0.22), 5(0.26, 0.31), 6(0.30, 0.31), 7(0.28, 0.36), and 8(0.39, 0.37).
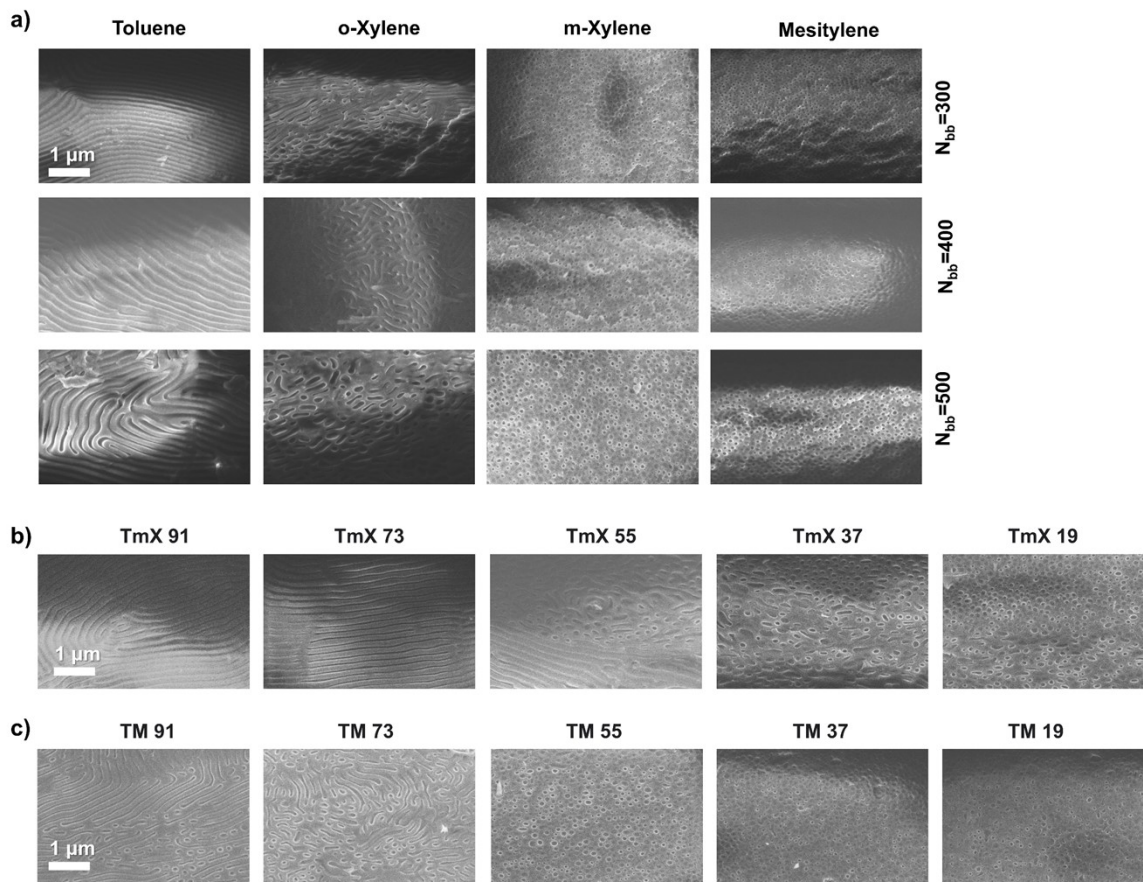
Figure S8. Analysis of structural characteristics of drop-casted samples based on different solvents and N_{bb}. **(a)** Vertical SEM image illustrating variations in nanostructures influenced by solvent choice and N_{bb} (300-500). The images demonstrate that increasing N_{bb} affects the size of the domain while preserving the phases. Vertical SEM image illustrating distinct nanostructures resulting from solvent composition variations: **(b)** toluene and m-xylene mixture, and **(c)** toluene and mesitylene mixture. The numerical notation denotes the volume ratio of each solvent (e.g., TmX73 = 70v% toluene with 30v% m-xylene). The scale remains consistent across all images.

1492 cm⁻¹ = aromatic stretching mode (C-C / C=C) in PS
1750 cm⁻¹ = carbonyl of the ester group in PLA

Figure S9. The Fourier transform infrared (FTIR) spectra of PLA (N_{bb}=200, N_{sc}=60, black), and PS (N_{bb}=200, N_{sc}=45, red) homobrush block copolymers. It represents both 1750 cm⁻¹ (carbonyl of the ester group in PLA), and 1492 cm⁻¹ (aromatic stretching mode in PS) peaks are mutually exclusive
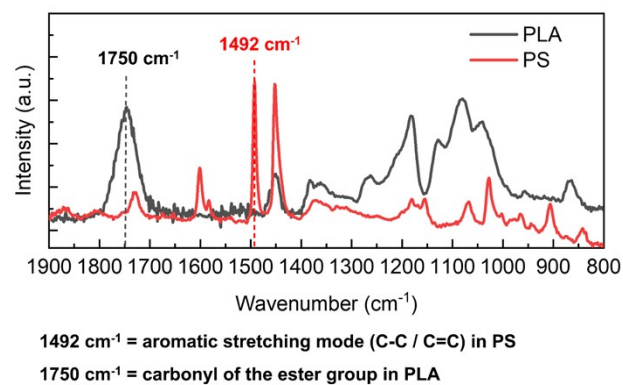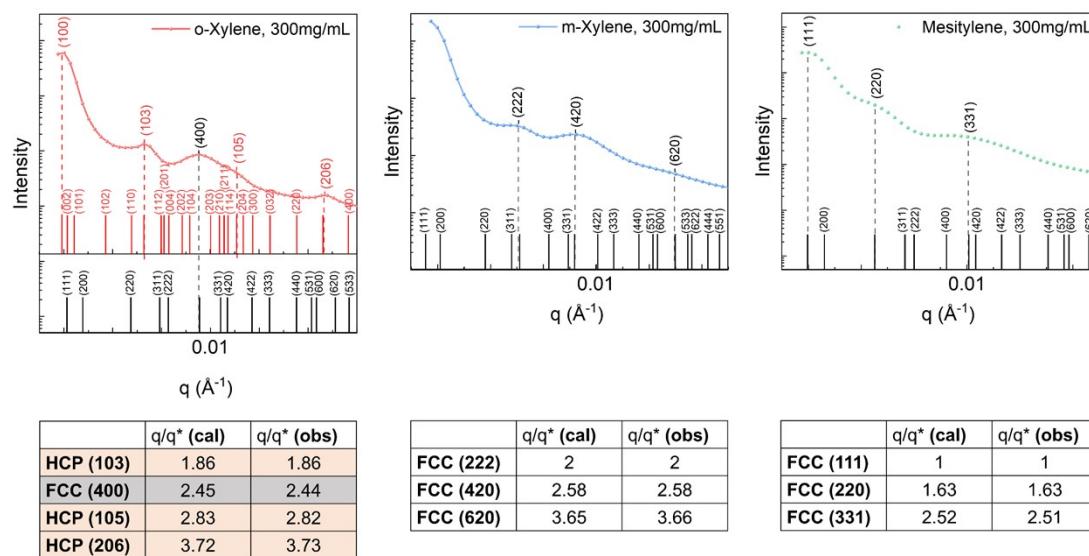
Figure S10. The Solution SAXS profiles BBCP at 300 mg/mL in **(a)** o-xylene, **(b)** m-xylene, and **(c)** mesitylene, with peak indexing (black: FCC, red: HCP). The table presents both the theoretically calculated $q/q*$ values and the observed $q/q*$ values of the peaks ($q*$: primary q-value; 391, 356, and 400 Å^{-1} for o-xylene, m-xylene, and mesitylene, respectively). All selective solvents display disordered close-packing structures. Specifically, o-xylene reveals peaks from a hybrid of FCC and HCP structures, while both m-xylene and mesitylene display peaks from a disordered FCC structure. The coexistence of both FCC and HCP phases is not unexpected, given their similar free energy and the sharing of the HCP (002) plane with the FCC (111) plane[3,4]. This coexistence is frequently observed, even in block copolymers[5].
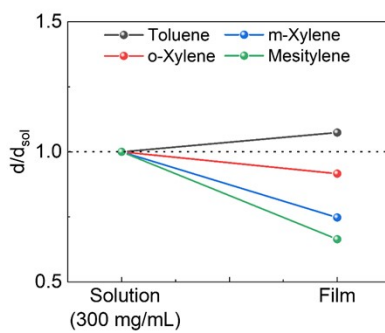
Figure S11. Analysis of Evaporation-driven domain size change. The y-axis reflects the ratio of domain size to the domain size of the concentrated solution at 300mg/mL (d_{sol}). Domain sizes were computed utilizing the primary q-value from the SAXS profile (**Figure 2b,** and **S10**).
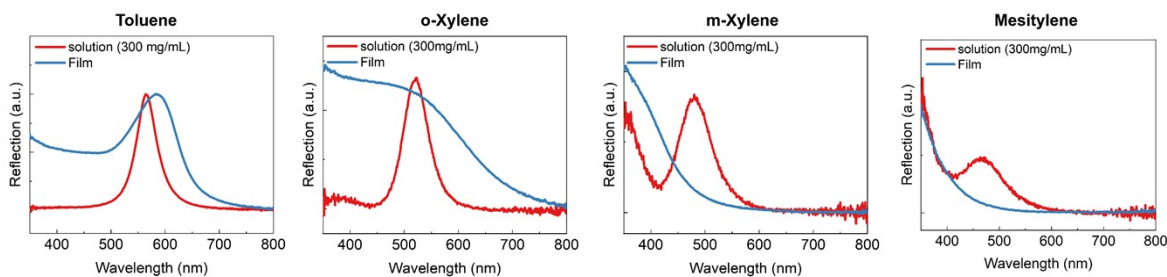
Figure S12. UV-Vis diffuse reflection spectra were measured for concentrated solutions (300 mg/mL) and drop-cast films from a solvent series. Solution samples were prepared by sandwiching the solution between two glass slides. The solutions exhibited sharp peaks across all solvents, while the films showed broad or absent peaks, indicating increased disorder upon solvent evaporation. These findings align with the SAXS results (**Figure 2**, and **3**) for both solution and film samples.
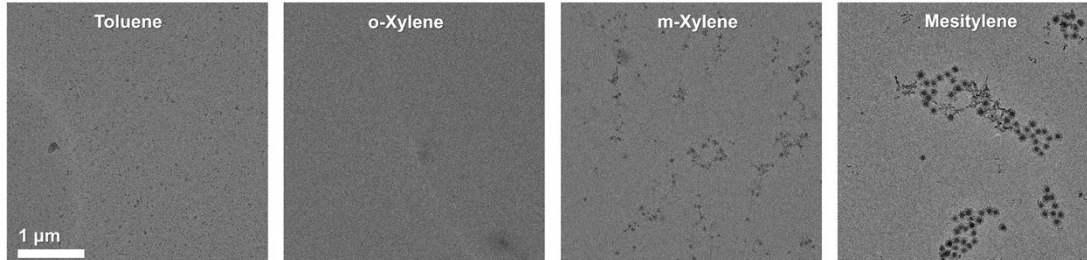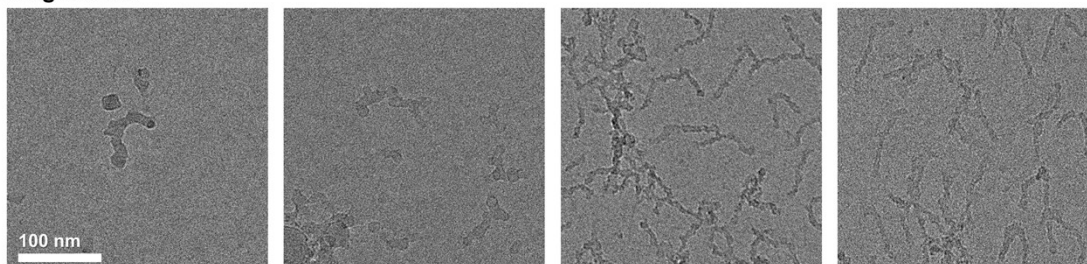
Figure S13. (a) TEM images of BBCP in four distinct solvents at a larger scale. There are no aggregation features visible in toluene and o-xylene. However, in m-xylene, aggregated particles are observed. Additionally, BBCP in mesitylene clearly showcases micelle formation. **(b)** TEM images focusing on BBCP single chains in each solvent. The scale remains consistent across all images.

Figure S14. SAXS fitting curves and data of 1 **(a, b, c,** and **d)** and 10 mg/mL **(e, f, g,** and **h)** solutions are depicted with raw data (black dots). For **(a, e)** toluene and **(b, f)** o-xylene, the flexible cylinder model was used for fitting (red curve). In the case of **(c, g)** m-xylene and **(d, h)** mesitylene, a hybrid model incorporating the core-shell model (blue curve) alongside the flexible cylinder model (green curve) was utilized for fitting. The red curves indicate the overall fitting curve. The tabulated values below represent the fitting results along with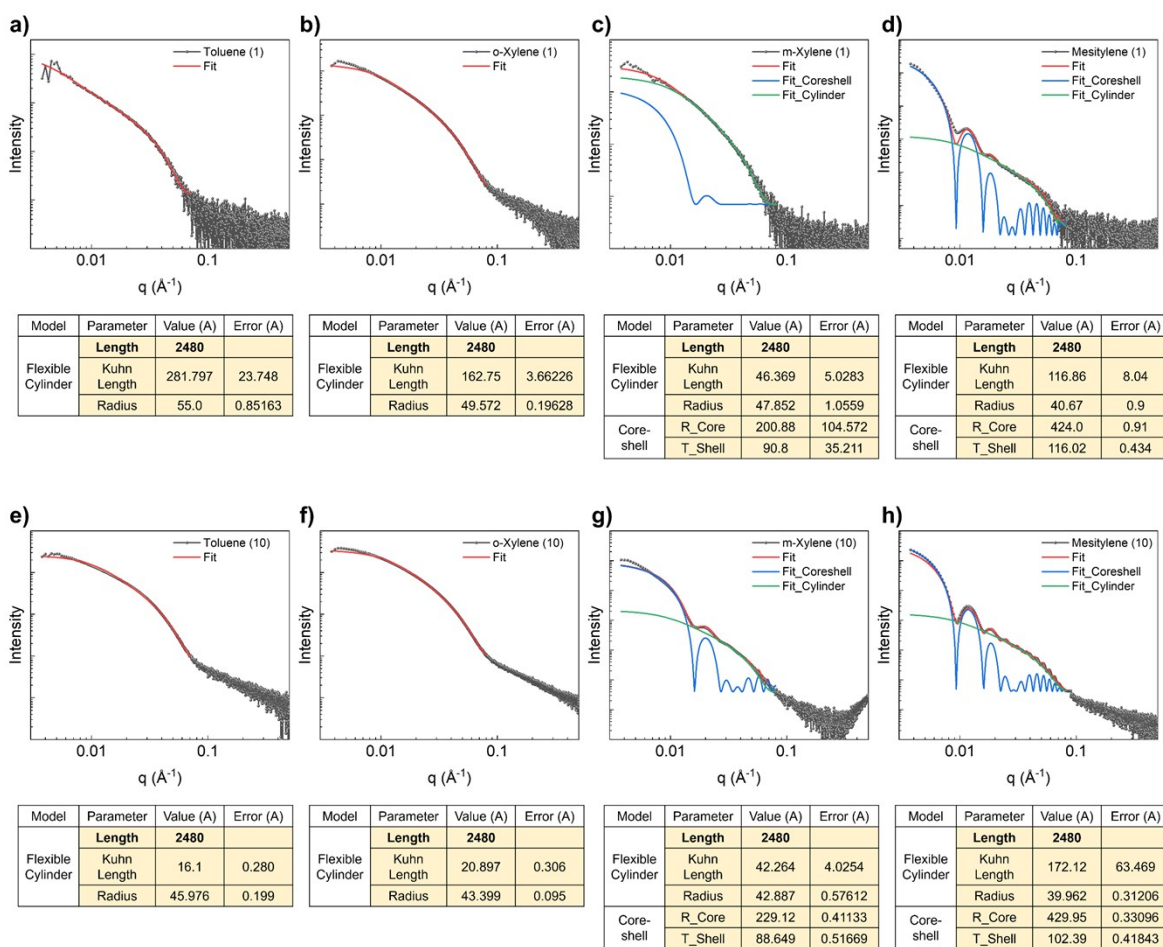 their respective errors. All the fitting curves closely match the data curves, and the estimated core-shell values align well with our observations in TEM.

a) Toluene (1)

Model	Parameter	Value (A)	Error (A)
Flexible Cylinder	Length	2480	
	Kuhn Length	281.797	23.748
	Radius	55.0	0.85163

b) o-Xylene (1)

Model	Parameter	Value (A)	Error (A)
Flexible Cylinder	Length	2480	
	Kuhn Length	162.75	3.66226
	Radius	49.572	0.19628

c) m-Xylene (1)

Model	Parameter	Value (A)	Error (A)
Flexible Cylinder	Length	2480	
	Kuhn Length	46.369	5.0283
	Radius	47.852	1.0559
Core-shell	R_Core	200.88	104.572
	T_Shell	90.8	35.211

d) Mesitylene (1)

Model	Parameter	Value (A)	Error (A)
Flexible Cylinder	Length	2480	
	Kuhn Length	116.86	8.04
	Radius	40.67	0.9
Core-shell	R_Core	424.0	0.91
	T_Shell	116.02	0.434

e) Toluene (10)

Model	Parameter	Value (A)	Error (A)
Flexible Cylinder	Length	2480	
	Kuhn Length	16.1	0.280
	Radius	45.976	0.199

f) o-Xylene (10)

Model	Parameter	Value (A)	Error (A)
Flexible Cylinder	Length	2480	
	Kuhn Length	20.897	0.306
	Radius	43.399	0.095

g) m-Xylene (10)

Model	Parameter	Value (A)	Error (A)
Flexible Cylinder	Length	2480	
	Kuhn Length	42.264	4.0254
	Radius	42.887	0.57612
Core-shell	R_Core	229.12	0.41133
	T_Shell	88.649	0.51669

h) Mesitylene (10)

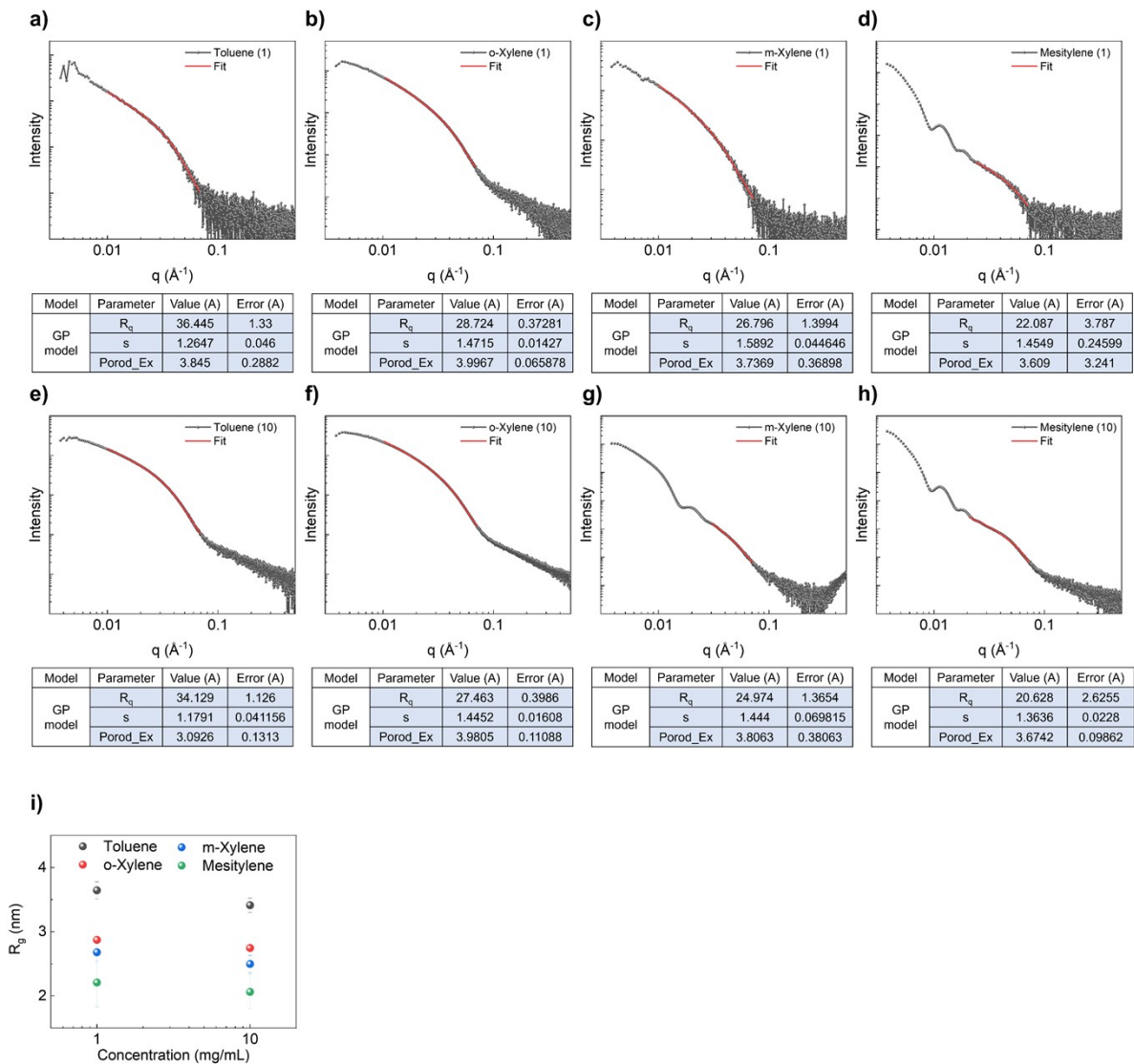| Model	Parameter	Value (A)	Error (A)
Flexible Cylinder	Length	2480	
	Kuhn Length	172.12	63.469
	Radius	39.962	0.31206
Core-shell	R_Core	429.95	0.33096
	T_Shell	102.39	0.41843

Figure S15. SAXS fitting curves (red curve) and data for both 1 (**a, b, c,** and **d**) and 10 mg/mL (**e, f, g,** and **h**) solutions are displayed with raw data indicated by black dots: **(a, e)** toluene, **(b, f)** o-xylene, **(c, g)** m-xylene, and **(d, h)** mesitylene. The curves were fitted within the range of the Guinier knee region (0.01-0.1 Å^{-1} range) using the Guinier-Porod model for each curve. The tabulated values below represent the fitting results along with their respective errors. **(i)** Estimated radius of gyration values of BBCP in different solvents (toluene: black, o-xylene: red, m-xylene: blue, and mesitylene: green) using SAXS model fitting at 1 and 10 mg/mL solution concentrations.

References

(1)   Wade, M. A.; Walsh, D.; Lee, J. C. W.; Kelley, E.; Weigandt, K.; Guironnet, D.; Rogers, S. A. Color, Structure, and Rheology of a Diblock Bottlebrush Copolymer Solution. *Soft Matter* **2020**, *16* (21), 4919–4931. https://doi.org/10.1039/d0sm00397b.

(2)   Walsh, D. J.; Guironnet, D. Macromolecules with Programmable Shape, Size, and Chemistry. *Proc Natl Acad Sci U S A* **2019**, *116* (5), 1538–1542. https://doi.org/10.1073/pnas.1817745116.

(3)   Woodcock, L. V. Entropy Difference between the Face-Centred Cubic and Hexagonal Close-Packed Crystal Structures. *Nature* **1997**, *385*, 141–143. https://doi.org/10.1038/385141a0.

(4)   Bolhuis, P. G.; Frenkel, D.; Mau, S.; Huse, D. A. Entropy Difference between Crystal Phases. *Nature* **1997**, *388*, 235–236. https://doi.org/10.1038/40779.

(5)   Zhang, C.; Vigil, D. L.; Sun, D.; Bates, M. W.; Loman, T.; Murphy, E. A.; Barbon, S. M.; Song, J. A.; Yu, B.; Fredrickson, G. H.; Whittaker, A. K.; Hawker, C. J.; Bates, C. M. Emergence of Hexagonally Close-Packed Spheres in Linear Block Copolymer Melts. *J Am Chem Soc* **2021**, *143* (35), 14106–14114. https://doi.org/10.1021/jacs.1c03647.